Published in final edited form as:
Magn Reson Med. 2014 June ; 71(6): 2035–2042. doi:10.1002/mrm.24868.

Dependence of blood T_2 on oxygenation at 7T: in vitro calibration and in vivo application

Lisa C. Krishnamurthy[1,2], **Peiying Liu**[1], **Feng Xu**[1], **Jinsoo Uh**[1], **Ivan Dimitrov**[1,3], and **Hanzhang Lu**[1]

[1]Advanced Imaging Research Center, University of Texas Southwestern Medical Center, Dallas, TX, USA

[2]Department of Biomedical Engineering, University of Texas at Arlington, Arlington, TX, USA

[3]Philips Medical Systems, Cleveland, OH, USA

Abstract

Purpose—The calibratable relationship between blood oxygenation (Y) and T_2 allows quantification of cerebral venous oxygenation. We aim to establish a calibration plot between blood T_2, Y, and hematocrit (Hct) at 7T, and using T_2-Relaxation-Under-Spin-Tagging (TRUST) MRI, determine human venous blood oxygenation *in vivo*.

Methods—*In vitro* experiments were performed at 7T on bovine blood samples using a CPMG-T_2 sequence, from which we characterized the relationship among T_2, Y, and Hct. TRUST MRI was implemented at 7T to measure venous blood T_2 *in vivo*, from which oxygenation was estimated using the *in vitro* calibration plot. Hyperoxia was performed to test the sensitivity of the method to oxygenation changes, and the 7T results were compared to those at 3T.

Results—*In vitro* data showed that arterial and venous T_2 at 7T are 68ms and 20ms, respectively, at a typical Hct of 0.42. *In vivo* measurement showed a cerebral venous oxygenation of 64.7±5.0% and a test-retest coefficient-of-variation of 3.6±2.4%. Hyperoxia increased Y_v by 9.0±1.4% (P=0.001) and the 3T and 7T results showed a strong correlation (R=0.95) across individuals.

Conclusion—We provided an *in vitro* calibration plot for conversion of blood T_2 to oxygenation at 7T and demonstrated its utility *in vivo*.

Keywords

blood oxygen saturation; blood T_2; 7T; TRUST; brain

Introduction

The knowledge of blood T_2 and its dependence on oxygenation (Y) have important implications in several MRI techniques such as interpretation of Blood-oxygenation-level-dependent (BOLD) fMRI signal (1,2), blood flow quantification in Arterial-Spin-Labeling

Corresponding author: **Name:** Hanzhang Lu, Ph.D. **Affiliations:** Advanced Imaging Research Center, Psychiatry, Radiology **Mailing Address:** UT Southwestern Medical Center 5323 Harry Hines Boulevard Dallas, Texas 75390 **Office Phone:** 214-645-2761 **Office Fax:** 214-645-2885 hanzhang.lu@utsouthwestern.edu.

(ASL) MRI (3), and for optimization of angiogram and venogram sequences (4). A particularly exciting application of this calibratable relationship is the quantification of venous oxygen saturation (Y_v) via the measurement of blood T_2 *in vivo* (5–17). These methods have demonstrated potential utilities in the normalization of fMRI signals (18), evaluation of brain metabolism (19), and understanding brain disorders (20). To date, all such studies have been performed at field strengths of 3T or lower.

Given that the susceptibility effect of deoxyhemoglobin increases with field strength (21–23), which has been one of the main motivations for high-field fMRI (23), it would be important to assess the potential of T_2-based oximetry techniques at 7T. It is well accepted that the blood T_2 is dependent on both Y and hematocrit (Hct) (24), since the modulation of either will cause a change in the local field. Blood T_2 at 7T has been measured for comparison of different biophysical models (11), but a complete calibration plot between T_2, Y, and Hct is not fully established at this field strength. The goals of the present study are therefore two-fold. First, we aim to obtain the relationship between blood T_2 and oxygenation at 7T (using *in vitro* blood sample experiment) in the context of various Hct levels. Second, we implemented a recently developed T2-Relaxation-Under-Spin-Tagging (TRUST) MRI technique at 7T and determined venous blood T_2 in human superior sagittal sinus. Utilizing the *in vitro* relationship as a calibration plot, we estimated global cerebral venous oxygenation. The technique was further evaluated using a hyperoxia maneuver to test its sensitivity to oxygenation changes. The 7T TRUST results were compared to those at 3T in the same participants.

Methods

In vitro study

In vitro experiments were performed on bovine blood (with 25 mM sodium citrate to avoid coagulation), which is known to have physiological and MR properties comparable to human blood (8,12,14,25,26). The blood was used on the same day that the sample was obtained from the local slaughter house. Experiments were performed on three pre-determined Hct levels that cover the normal range of this parameter (Hct = 34%, 42%, 54%). At each Hct, 10–18 oxygenation levels (range 27–100%) were assessed, and they are completed using 2–3 batches of blood. Hct was adjusted by adding or removing plasma after spinning the blood samples in a centrifuge at 2500 RPM for 30 minutes. The oxygenation of the sample was modulated with exposure to room air or a nitrogen atmosphere. Oxygenation and Hct were measured using a blood gas analyzer (Radiometer ABL80 FLEX, Copenhagen, Denmark).

Blood samples were placed in 27 mm plastic tubes and scanned using a small animal 7T (16-cm horizontal bore) MR scanner (Varian Inc, Palo Alto, CA) with a 38 mm birdcage RF coil. The temperature of the blood was controlled by initially placing the tubes in a 37°C water bath while gently agitating the sample to keep the erythrocytes in suspension. The sample was then transferred to the scanner, where the ambient temperature of the magnet bore was maintained at 37°C with heated air on a temperature-controlled feedback loop. The blood T_2 was measured with a Carr-Purcell-Meiboom-Gill (CPMG) T_2 spectroscopy sequence (27,28) with τ_{CPMG} = 5 ms and effective echo time (eTE) = 10, 20, 40, 80, 160,

and 320 ms, corresponding to 2, 4, 8, 16, 32, and 64 hard refocusing pulses (180° pulse = 235 μs pulse duration), TR = 15,000 ms, 2 averages, and scan duration = 3 minutes. Estimation of T_2 was based on standard mono-exponential fitting and the goodness-of-fit was evaluated by a Matlab (Mathworks, Natick, MA) function, nlparci, which provides the standard error (=95% confidence interval/2/1.96) of the parameter estimation. The blood T_2 was measured twice on each Hct-Y combination, and the second measurement was constrained to provide a T_2 value that was within 1 ms of the first measurement. If not, the sample was agitated and the T_2 measured again, in case precipitation had occurred during the scan. We note that we only had to re-agitate the sample in 2 out of 40 measurement sessions. Thus, the precipitation effect within the 6-minute session (3 minutes × 2) is minimal. This is also consistent with the relatively slow sedimentation rate of erythrocyte of approximately 1 mm/hour (29,30).

To establish the calibration plot, we first fitted the T_2-Y data at each Hct value to a model proposed by Wright et al. (7) and Golay et al. (8) :

$$\frac{1}{T_2}=A+B\cdot(1-Y)+C\cdot(1-Y)^2 \quad [1]$$

where *A*, *B*, and *C* are coefficients estimated from the data fitting. Linear interpolation of each coefficient was then used to cover the entire range of Hct. With this procedure, we obtained a 3D plot completely characterizing the relationship among T_2, Y, and Hct.

In vivo study: general procedures

In vivo study was performed on a 7 Tesla whole-body MRI scanner (Achieva, Philips Medical Systems, Best, The Netherlands). The protocol was approved by the University of Texas Southwestern Medical Center's Institutional Review Board. RF transmission and reception was achieved via a volume Transmit/Receive head coil (Nova Medical Inc, Wilmington, MA), where quadrature was used for transmission, and 16 channels were used for receiving. The subjects were instructed not to fall asleep (verified after the scan), and foam padding was placed around the head to minimize motion.

The placement of the imaging and labeling slab for 7T TRUST is depicted in Figure 1a, where the yellow rectangle represents the imaging slab, and the green rectangle represents the labeling slab. The pulse sequence diagram of the 7T TRUST is similar to the one previously developed at 3T (5,6) and is illustrated in Fig. 1b. It applies the spin labeling principle (red-box) on the venous side and acquires control and labeled images, the subtraction of which yields pure venous blood signal (5). T_2 value of the pure venous blood was then determined using non-selective T_2-preparation pulses (blue-box), minimizing the effect of flow on T_2 estimation. Due to relatively large flow velocities, TRUST measurements in large venous vessels, e.g. sagittal sinus, was found to be particularly robust, and was thus chosen as the vessel-of-interest in the present study. A pre-saturation pulse train (green-box) is applied on the imaging plane to suppress static tissue signal using a Water suppression Enhanced through T_1 effects (WET) scheme (τ_{WET} = 10 ms, θ_1 = 106.8°, θ_2 = 86.8°, θ_3 = 76.0°, θ_4 = 153.6°) (31,32). A non-selective post-saturation pulse train (black-box) is used to “reset” the magnetization of all spins, which was shown to

improve the measurement accuracy in TRUST (6) and other sequences (33–35). Single slice acquisition (orange-box) used a single-shot gradient-echo EPI.

The T_2-preparation incorporated hard composite refocusing pulses (90_x-180_y-90_x) using a MLEV-16 phase cycling scheme (36), which requires that a multiple of four refocusing pulses be used in order to minimize the effect of imperfection in flip angle (due to B_1 and B_0 inhomogeneities). We used τ_{CPMG} = 5 ms (Figure 1, blue-box) to match our *in vitro* blood calibration curve. Two eTEs of 20 and 40 ms (composed of 4 and 8 refocusing pulses respectively) were used, since the blood T_2 at the target Hct-Y combination is short and a larger number of refocusing pulses (e.g. 12, 16, etc) would result in excessively diminished signal. Other imaging parameters are as follows: FOV = 220 × 220 mm^2, Acquisition matrix = 64 × 64, in-plane resolution 3.4 × 3.4 mm^2, half-scan factor = 0.636, SENSE factor = 3 (AP), echo time (TE) = 2.7 ms, 1 slice, slice thickness = 5 mm, TR = 3.3 sec, inversion time (TI) = 800 ms, label thickness = 100 mm, label gap (between imaging and label slab) = 22.5 mm, head SAR = 3.7 W/kg, 16 averages, scan duration = 3.5 minutes. The imaging slice is placed parallel to the AC-PC line, 30 mm above the draining vessel's confluence point.

In vivo study design

A total of 24 subjects were scanned, and were categorized into one of three study sub-groups: feasibility, reproducibility, or sensitivity study. Feasibility of the proposed TRUST sequence was tested in an initial sub-group of 15 participants (age 31±8 years, range 23–54, 11 Males). Reproducibility of the TRUST protocol was evaluated in a second sub-group of 5 subjects (age 33±4 years, range 27–39, 4 Males), by repeating the scan 5 times in one session. Coefficient of Variation (CoV) was calculated based on standard deviation of the multiple scans divided by their mean.

Sensitivity of the technique to oxygenation changes was tested by inducing hyperoxia in a third sub-group of 4 subjects (age 33±8 years, range 26–41, 3 Males) (37). For verification of the 7T results, we also performed the TRUST scans on a 3T (Achieva, Philips Medical Systems, Best, The Netherlands), which we have validated previously (26). The 3T protocol and imaging parameters were similar to an optimized protocol (38), though some parameters were altered to match the 7T protocol in scan duration (TR=3.3 sec, TI=1064 ms, 64 dynamics, 8 averages). This resulted in matched scan duration of 3.5 minutes at both field strengths. Each subject was scanned on both 7T and 3T on the same day, the order of which was counterbalanced across participants. On each scanner, a baseline (normoxia) TRUST scan was conducted while the subject breathed room-air. Then, without repositioning the subject, hyperoxia was induced by having the subject inhale a gas mixture of 98% O_2 and 2% CO_2, using procedures described previously (37). The small amount of CO_2 was added to offset the subject hyperventilation and to maintain the constant end-tidal CO_2 (37). After switching the gas, a 3 minute waiting period was used to allow the subject's physiology to stabilize, after which a TRUST scan under hyperoxic state was conducted. Vital signs including end-tidal O_2, and end-tidal CO_2 were continuously monitored during the entire session. After all scans, 5cc of blood was drawn from the arm to determine the subject's Hct using a micro-centrifuge (Hemata STAT II, Separation Technology, Inc., Altamonte

Springs, FL, USA). Comparison between results at the two field strengths was conducted using scatter plot, paired Student t-test, and Pearson correlation coefficient.

In vivo MRI Data Analysis

The *in vivo* imaging data was analyzed using in-house Matlab (Mathworks Inc, Natick, MA) codes as described previously (5). Briefly, a difference image between control and label images was computed. The four voxels in the sagittal sinus with the largest difference signal were included in the ROI mask. The averaged signal in the mask was fitted to a mono-exponential function of eTE to obtain the decay constant, *d*. Blood T_2 was then calculated by $1/T_2 = d + 1/T_1$. We point out that, since blood T_1 at 7T (~2100ms (39–41)) is more than 20 times greater than T_2, the impact of the T_1 variation is minimal. Note that, in this study, we delineated the vessel voxels using the TRUST difference image instead of a separate anatomic image. The reason is that voxel masks defined on anatomic image may not be readily applicable to the TRUST data due to several factors including differences in spatial resolution, EPI distortion in the TRUST images, and potential subject motion between the TRUST and anatomic scans.

Results

In vitro T_2 relaxometry

The in vitro data resulted in reliable T_2 fittings. The standard error of the estimated R_2 ($=1/T_2$) was 1.1±1.4 Hz (mean±sd, range 0.1–6.0 Hz, N=40). Figure 2a shows the *in vitro* blood T_2 versus Y at each Hct level. There is a minor influence from Hct, with major changes in T_2 resulting from changes in Y. The constants for Equation [1] can be found in Table 1. Linear interpolation of each coefficient can be used to describe T_2-relaxometry at other Hct values. At a typical Hct level of 0.42, arterial (assuming 100% oxygenation) and venous (assuming 60% oxygenation) blood T_2 are expected to be 68 ms and 20 ms, respectively. Comparing to lower field strengths of 3T (26) and 1.5T (13), the blood R_2 ($=1/T_2$) at 7T (acquired in this study) changes much more rapidly with Y (Figure 2b). Similar field-dependent curves for blood R_2* have been shown by Blockley, et al. (40).

In vivo study

Figure 3 shows a representative TRUST dataset at 7T. TRUST MRI results in a label and control image for each eTE, which are then magnitude subtracted to provide a difference image of pure blood signal (Figure 3a). Note that the blood signal in the target vessel, the superior sagittal sinus, is quite robust and decays with T_2-preparation duration (eTE), allowing for a reliable R_2 fitting (Figure 3b). The standard error of the R_2 estimation was 4.8 ± 2.3 Hz. Of the 15 subjects scanned for the feasibility test, the blood T_2 was 25.0 ± 4.8 ms (Mean ± STD). Using the *in vitro* calibration plot established above, these T_2 values were converted to Y_v of 64.7 ± 5.0%.

The reproducibility of TRUST at 7T was investigated by repeating the protocol 5 times in a single session in a group of subjects. CoV of the measurements was 3.6 ± 2.4%, which is larger than the 3T TRUST CoV of 1.9 ± 0.6 % reported in the literature (38), but is still relatively small compared to normal variation of human Y_v from 50–75% (42). The effect of

ROI size was tested by varying the number of selected voxels from 1 to 6, and it was found that the estimated T_2 was not dependent on the ROI size, consistent with previous observations at 3T (5).

Data from the physiologic challenge study are summarized in Table 2. TRUST scans at the 7T showed that hyperoxia maneuver increased Y_v by 9.0 ± 1.4 % (Mean ± STD, P=0.001), which is consistent with the 10.6% increase reported in the literature using a similar gas mixture (37). The 7T results were also supported by the 3T data collected in the same subjects, which showed an 8.3 ± 1.0 % increase in Y_v. The increase in Y_v measured at 3T was not significantly different than 7T, as evaluated with a paired t-test (P = 0.57). Furthermore, the 3T and 7T Y_v results are significantly (R=0.95, P=0.0004) correlated across individuals (Figure 4). There was no difference in the Y_v values measured at 3T versus 7T (P=0.77), and their regression slope was close to unity (slope=0.998).

Discussion

The present study showed that blood CPMG-T_2 at 7T is dependent on both hematocrit and oxygenation levels, the slope of which is greater than those at lower fields. Using this relationship as a calibration plot, venous oxygenation in the human brain can be estimated *in vivo*. The oxygenation values measured at 7T were in excellent agreement with the 3T results and also showed a strong sensitivity to oxygenation changes induced by hyperoxia.

Dependence of blood T_2 and T_2* on oxygenation has been well established at 1.5T (7,12,13,32,43), and 3T (14,26,43), but the literature at 7T is not extensive. The only report we are aware of on CPMG-T_2 at 7T is the study of Gardener et al. (11), who compared the exchange and diffusion models in describing the T_2 relaxation process in blood. In the present study, blood T_2 was only measured at a τ_{CPMG} = 5 ms, since our goal is to provide a calibration plot rather than performing an investigation of biophysical modeling. We compared the T_2 values (at τ_{CPMG} = 5 ms) and their dependence on oxygenation between the two studies. T_2 of fully oxygenated blood in the present study and Gardener et al. is 68 ms and 64 ms, respectively, showing good agreement. The values, however, showed some discrepancy for less oxygenated blood. Specifically, the T_2 data from the present study revealed a stronger dependence on oxygenation (solid blue curve in Figure 2c), compared to the data in the earlier study (dashed blue curve in Figure 2c). One possible reason for the discrepancy is the condition of the blood samples used. In all of our experiments, the blood samples were scanned within 5 hours of collection from the animal, thus the fraction of lysed cells is expected to be minimal. In the earlier study, blood samples up to 48 hours after drawing were used, and the likelihood of cell lysing is greater. Lysed cells are known to be associated with a longer T_2 (23). Our testing showed that, for fully oxygenated blood, T_2 of lysed cells is approximately 20% greater than that of whole blood. For venous blood oxygenation, this difference could be more than 90%. Note also that this effect is expected to be present at all field strengths. Another potential reason is the species-dependent differences in blood properties. The present study used bovine blood, as opposed to human blood used by Gardener, et al. However, we point out that bovine blood has been widely used in previous T_2-relaxometry studies (8,10,14,26,39,44,45) and has been shown to be valid for human data calibration (8,9,16,26), mainly because its physiologic and MR

properties are comparable to human blood (25). Thus, the effect of species difference is expected to be relatively small. There are other factors that could affect the estimated T_2 values, such as sample preparation, the actual degree of the refocusing pulse angles, and details of the pulse sequences. We would like to point out that our *in vivo* data appears to support the *in vitro* results, in that the estimated venous oxygenation values using the *in vitro* calibration plot are well within the expected range and are in excellent agreement with the 3T results. We have also tested the calibration plot by Gardener et al. to calibrate our *in vivo* data. We found a normoxia venous oxygenation of 19.3% and a hyperoxia oxygenation of 44.3%, which are considerably lower than the present 3T results and the normoxia literature values of 58.4–67.1% (5,8,15,17,19,37,38,46–51) and hyperoxia literature values of 75.5% (37).

To our knowledge, the present study is the first report to quantitatively evaluate blood oxygenation in humans at 7T. Our observed venous oxygenation at 7T was within the expected range, and was further supported by the 3T results, which suggests that *in vivo* measurement of blood T_2 at 7T is feasible. Although this study has primarily focused on a global oxygenation technique, it should be noted that the T_2-versus-oxygenation relationship provided in the present study is not limited to TRUST application, but can also be used for calibration of other T_2-based oximetry techniques, such as QUIXOTIC (16), VSEAN (17), TRU-PC (15,52), and IQ-OEF (53). It should also be mentioned that other oximetry techniques that do not require T_2-calibration are available. These methods include quantitative Blood-Oxygenation-Level-Dependent (qBOLD) contrast (46,50,54,55), susceptibility phase based techniques (47–49,51), gas inhalation techniques (56–58), and quantitative susceptibility mapping (QSM) methods (59). Most of these techniques may also benefit from the increased field strength at 7T.

Comparing T_2 oximetry between 7T and 3T, the higher field strength provides certain advantages, but also presents new challenges. The advantages associated with the higher field include greater intrinsic SNR and increased susceptibility effects of deoxyhemoglobin, which results in a steeper dependence of blood R_2 on oxygenation. However, greater B_0 and B_1 inhomogeneities at higher fields also bring several obstacles. For example, we were not able to use an eTE of 0 ms (i.e. tip-down followed immediately by tip-up pulse) when the signal is supposedly the strongest. This is because there is a finite amount of time (~0.6 ms) between the tip-down and tip-up pulse, which causes the magnetization to rotate away from the original axis when the spin is off-resonance. Thus, the tip-up pulse is not able to return all of the magnetization back to the longitudinal direction. This effect manifests itself as an eTE=0 signal that is consistently lower than the fitting curve. Therefore, the shortest TE we could use in this 7T study was eTE = 20 ms. Note that this factor by itself reduced our starting SNR by approximately 63% (assuming a blood T_2 of 20 ms). We believe this was a major reason for the larger variability of our 7T data compared to previous 3T results (38). Another issue is that we were not able to use a long eTE of 80 ms, because the signal would have decayed too much (to about 2% of the original signal) considering a blood T_2 of 20 ms. As a consequence of both effects, our 7T protocol used two eTE values corresponding to 4 and 8 refocusing pulses, as opposed to our standard 3T protocol in which we use four eTE values corresponding to 0, 4, 8, and 16 refocusing pulses. As a simple demonstration, we

took the 3T TRUST reproducibility data (CoV quoted at 1.88% (38)) and re-analyzed the data by excluding eTE 0 and 160 ms. The new average intra-session CoV at 3T becomes 4.3±3.7%, which is larger than the 7T CoV of 3.6±2.4%. Therefore, future efforts for 7T T_2-based oximetry should emphasize the improvement of B_0 and B_1 homogeneity. For small vessel techniques, it may be helpful to use local volume shimming or apply dielectric bags for these purposes (60). Additionally, SAR is greater at 7T, which increased our TR (to 3300 ms) compared to the optimized TR of 3000 ms at 3T. B_1 shimming may be useful to reduce the SAR constraints.

A limitation of the present study is that the *in vivo* and *in vitro* data were acquired on different MRI systems. We chose to perform the *in vitro* study on an animal system, because the B_1 and B_0 inhomogeneities will be minimized in the smaller bore of the animal system. However, since the MRI systems were different, the resulting pulse sequences, in particular the T_2-preparation pulses, were not exactly matched. This raised the question whether it is valid to use the *in vitro* data to calibrate the *in vivo* T_2 in our results. We therefore conducted additional experiments on the 3T to verify the 7T Y_v values. The excellent agreement between the 7T and 3T data (Figure 4) suggests that the calibration results were generally acceptable. We speculate that two processes in the human 7T MRI system may be in play concomitantly, and their consequences in biasing T_2 estimation partially cancel out. One is that the human 7T sequence used a composite refocusing pulse, which is known to result in a longer apparent T_2. The other is that human 7T imaging is known to suffer from B_1 inhomogeneity, the consequence of which is a shortened apparent T_2. We did not perform a dedicated B_1 map in our study. However, using signal intensities in the TRUST images, we estimated that the B_1^+ field in the sagittal sinus area was 83±2% (mean±SD, N=5) of the nominal value. According to our simulation, the effect of this reduced B_1^+ in combination with the pulse width effect will yield a T_2 that is 94±7% of the true T_2. Future study using B_1 mapping and, preferably, improved B_1 homogeneity is needed to verify these predictions.

Conclusion

We characterized the relationship between blood T_2, oxygenation, and Hct at the field strength of 7T, thereby providing a foundation for future experimental or simulation studies that may benefit from this information. We also reported the first study to quantitatively estimate blood oxygenation in human brain at 7T and verified the results with 3T experiments.

Acknowledgments

The authors would like to thank Dr. Ksenija Grgac for invaluable information on performing *in vitro* blood experiments. We would also like to thank the faculty and staff of the Advanced Imaging Research Center for all of their help and resources, especially Dr. Kim Kangasniemi and Charles “Chuck” Storey for great support on the blood experiments.

Grant Sponsors: NIH R01 MH084021, NIH R01 NS067015, NIH R01 AG042753, NIH R21 NS078656

References

1. Duong TQ, Yacoub E, Adriany G, Hu X, Ugurbil K, Kim SG. Microvascular BOLD contribution at 4 and 7 T in the human brain: gradient-echo and spin-echo fMRI with suppression of blood effects. Magn Reson Med. 2003; 49(6):1019–1027. [PubMed: 12768579]
2. Yacoub E, Duong TQ, Van De Moortele PF, Lindquist M, Adriany G, Kim SG, Ugurbil K, Hu X. Spin-echo fMRI in humans using high spatial resolutions and high magnetic fields. Magn Reson Med. 2003; 49(4):655–664. [PubMed: 12652536]
3. Parkes LM. Quantification of cerebral perfusion using arterial spin labeling: two-compartment models. J Magn Reson Imaging. 2005; 22(6):732–736. [PubMed: 16267854]
4. Du YP, Jin Z, Hu Y, Tanabe J. Multi-echo acquisition of MR angiography and venography of the brain at 3 Tesla. J Magn Reson Imaging. 2009; 30(2):449–454. [PubMed: 19629975]
5. Lu H, Ge Y. Quantitative evaluation of oxygenation in venous vessels using T2-Relaxation-Under-Spin-Tagging MRI. Magn Reson Med. 2008; 60(2):357–363. [PubMed: 18666116]
6. Xu F, Uh J, Liu P, Lu H. On improving the speed and reliability of T2-relaxation-under-spin-tagging (TRUST) MRI. Magn Reson Med. 2011; 68(1):198–204. [PubMed: 22127845]
7. Wright GA, Hu BS, Macovski A. 1991 I.I. Rabi Award. Estimating oxygen saturation of blood in vivo with MR imaging at 1.5 T. J Magn Reson Imaging. 1991; 1(3):275–283. [PubMed: 1802140]
8. Golay X, Silvennoinen MJ, Zhou J, Clingman CS, Kauppinen RA, Pekar JJ, van Zij PC. Measurement of tissue oxygen extraction ratios from venous blood T(2): increased precision and validation of principle. Magn Reson Med. 2001; 46(2):282–291. [PubMed: 11477631]
9. Oja JM, Gillen JS, Kauppinen RA, Kraut M, van Zijl PC. Determination of oxygen extraction ratios by magnetic resonance imaging. J Cereb Blood Flow Metab. 1999; 19(12):1289–1295. [PubMed: 10598932]
10. Qin Q, Grgac K, van Zijl PC. Determination of whole-brain oxygen extraction fractions by fast measurement of blood T(2) in the jugular vein. Magn Reson Med. 2011; 65(2):471–479. [PubMed: 21264936]
11. Gardener AG, Francis ST, Prior M, Peters A, Gowland PA. Dependence of blood R2 relaxivity on CPMG echo-spacing at 2.35 and 7 T. Magn Reson Med. 2010; 64(4):967–974. [PubMed: 20715058]
12. Silvennoinen MJ, Clingman CS, Golay X, Kauppinen RA, van Zijl PC. Comparison of the dependence of blood R2 and R2* on oxygen saturation at 1.5 and 4.7 Tesla. Magn Reson Med. 2003; 49(1):47–60. [PubMed: 12509819]
13. Stefanovic B, Pike GB. Human whole-blood relaxometry at 1.5 T: Assessment of diffusion and exchange models. Magn Reson Med. 2004; 52(4):716–723. [PubMed: 15389952]
14. Zhao JM, Clingman CS, Narvainen MJ, Kauppinen RA, van Zijl PC. Oxygenation and hematocrit dependence of transverse relaxation rates of blood at 3T. Magn Reson Med. 2007; 58(3):592–597. [PubMed: 17763354]
15. Jain V, Magland J, Langham M, Wehrli FW. High temporal resolution in vivo blood oximetry via projection-based T(2) measurement. Magn Reson Med. in press: doi 10.1002/mrm.24519.
16. Bolar DS, Rosen BR, Sorensen AG, Adalsteinsson E. QUantitative Imaging of eXtraction of oxygen and TIssue consumption (QUIXOTIC) using venular-targeted velocity-selective spin labeling. Magn Reson Med. 2011; 66(6):1550–1562. [PubMed: 21674615]
17. Guo J, Wong EC. Venous oxygenation mapping using velocity-selective excitation and arterial nulling. Magn Reson Med. 2012; 68(5):1458–1471. [PubMed: 22294414]
18. Lu H, Zhao C, Ge Y, Lewis-Amezcua K. Baseline blood oxygenation modulates response amplitude: Physiologic basis for intersubject variations in functional MRI signals. Magn Reson Med. 2008; 60(2):364–372. [PubMed: 18666103]
19. Xu F, Ge Y, Lu H. Noninvasive quantification of whole-brain cerebral metabolic rate of oxygen (CMRO2) by MRI. Magn Reson Med. 2009; 62(1):141–148. [PubMed: 19353674]
20. Ge Y, Zhang Z, Lu H, Tang L, Jaggi H, Herbert J, Babb JS, Rusinek H, Grossman RI. Characterizing brain oxygen metabolism in patients with multiple sclerosis with T2-relaxation-under-spin-tagging MRI. J Cereb Blood Flow Metab. 2012; 32(3):403–412. [PubMed: 22252237]

21. Fabry ME, San George RC. Effect of magnetic susceptibility on nuclear magnetic resonance signals arising from red cells: a warning. Biochemistry. 1983; 22(17):4119–4125. [PubMed: 6615821]
22. Matwiyoff NA, Gasparovic C, Mazurchuk R, Matwiyoff G. On the origin of paramagnetic inhomogeneity effects in whole blood. Magn Reson Med. 1991; 20(1):144–150. [PubMed: 1658536]
23. Thulborn KR, Waterton JC, Matthews PM, Radda GK. Oxygenation dependence of the transverse relaxation time of water protons in whole blood at high field. Biochim Biophys Acta. 1982; 714(2):265–270. [PubMed: 6275909]
24. van Zijl PC, Eleff SM, Ulatowski JA, Oja JM, Ulug AM, Traystman RJ, Kauppinen RA. Quantitative assessment of blood flow, blood volume and blood oxygenation effects in functional magnetic resonance imaging. Nat Med. 1998; 4(2):159–167. [PubMed: 9461188]
25. Benga G, Borza T. Diffusional water permeability of mammalian red blood cells. Comp Biochem Physiol B Biochem Mol Biol. 1995; 112(4):653–659. [PubMed: 8590380]
26. Lu H, Xu F, Grgac K, Liu P, Qin Q, van Zijl P. Calibration and validation of TRUST MRI for the estimation of cerebral blood oxygenation. Magn Reson Med. 2012; 67(1):42–49. [PubMed: 21590721]
27. Carr HY, Purcell EM. Effects of Diffusion on Free Precession in Nuclear Magnetic Resonance Experiments. Phys Rev. 1954; 94(3):630–638.
28. Meiboom S, Gill D. Modified Spin-Echo Method for Measuring Nuclear Relaxation Times. The Review of Scientific Instruments. 1958; 29(8):688–691.
29. Eliasson R, Samelius-Broberg U. The effect of dextran and some other colloids on the suspension stability of blood from different species. Acta Physiol Scand. 1965; 64(3):245–250. [PubMed: 4159169]
30. Taimur MJFA, Halder AK, Chowdhury SMZH, Akhter N, Islam MS, Kamal AHM, Islam KS. Hematological studies on cattle exposed to fasciola gigantica infestation. Asian-Australasian Journal of Animal Sciences. 1993; 6(2):301–303.
31. Ogg RJ, Kingsley PB, Taylor JS. WET, a T1- and B1-insensitive water-suppression method for in vivo localized 1H NMR spectroscopy. J Magn Reson B. 1994; 104(1):1–10. [PubMed: 8025810]
32. Golay X, Petersen ET, Hui F. Pulsed star labeling of arterial regions (PULSAR): a robust regional perfusion technique for high field imaging. Magn Reson Med. 2005; 53(1):15–21. [PubMed: 15690497]
33. Pell GS, Thomas DL, Lythgoe MF, Calamante F, Howseman AM, Gadian DG, Ordidge RJ. Implementation of quantitative FAIR perfusion imaging with a short repetition time in time-course studies. Magn Reson Med. 1999; 41(4):829–840. [PubMed: 10332861]
34. Lu, H. Magnetization “Reset” for Non-Steady-State Blood Spins in Vascular-Space-Occupancy (VASO) fMRI. 16th Annual Proceedings of International Society for Magnetic Resonance in Medicine Toronto; Canada. 2008. p. 406
35. Wu WC, Buxton RB, Wong EC. Vascular space occupancy weighted imaging with control of residual blood signal and higher contrast-to-noise ratio. IEEE Trans Med Imaging. 2007; 26(10): 1319–1327. [PubMed: 17948723]
36. Levitt MH, Freeman R, Frenkiel T. Broadband Heteronuclear Decoupling. J Magnetic Res. 1982; 47:328–330.
37. Xu F, Liu P, Pascual JM, Xiao G, Lu H. Effect of hypoxia and hyperoxia on cerebral blood flow, blood oxygenation, and oxidative metabolism. J Cereb Blood Flow Metab. 2012; 32(10):1909–1918. [PubMed: 22739621]
38. Liu P, Xu F, Lu H. Test-retest reproducibility of a rapid method to measure brain oxygen metabolism. Magn Reson Med. 2013; 69(3):675–681. [PubMed: 22517498]
39. Grgac K, van Zijl PC, Qin Q. Hematocrit and oxygenation dependence of blood (1) H(2) O T(1) at 7 tesla. Magn Reson Med. in press; doi 10.1002/mrm.24547.
40. Blockley NP, Jiang L, Gardener AG, Ludman CN, Francis ST, Gowland PA. Field strength dependence of R1 and R2* relaxivities of human whole blood to ProHance, Vasovist, and deoxyhemoglobin. Magn Reson Med. 2008; 60(6):1313–1320. [PubMed: 19030165]

41. Dobre MC, Ugurbil K, Marjanska M. Determination of blood longitudinal relaxation time (T1) at high magnetic field strengths. Magn Reson Imaging. 2007; 25(5):733–735. [PubMed: 17540286]
42. Kety S, Schmidt C. The Effects of Altered Arterial Tension of Carbon Dioxide and Oxygen on Cerebral Blood Flow and Cerebral Oxygen Consumption of Normal Young Men. J Clin Invest. 1948; 27:484–492. [PubMed: 16695569]
43. Chen JJ, Pike GB. Human whole blood T2 relaxometry at 3 Tesla. Magn Reson Med. 2009; 61(2): 249–254. [PubMed: 19165880]
44. Lu H, Clingman C, Golay X, van Zijl PC. Determining the longitudinal relaxation time (T1) of blood at 3.0 Tesla. Magn Reson Med. 2004; 52(3):679–682. [PubMed: 15334591]
45. Meyer ME, Yu O, Eclancher B, Grucker D, Chambron J. NMR relaxation rates and blood oxygenation level. Magn Reson Med. 1995; 34(2):234–241. [PubMed: 7476083]
46. An H, Lin W. Quantitative measurements of cerebral blood oxygen saturation using magnetic resonance imaging. J Cereb Blood Flow Metab. 2000; 20(8):1225–1236. [PubMed: 10950383]
47. Fan AP, Benner T, Bolar DS, Rosen BR, Adalsteinsson E. Phase-based regional oxygen metabolism (PROM) using MRI. Magn Reson Med. 2012; 67(3):669–678. [PubMed: 21713981]
48. Fernandez-Seara MA, Techawiboonwong A, Detre JA, Wehrli FW. MR susceptometry for measuring global brain oxygen extraction. Magn Reson Med. 2006; 55(5):967–973. [PubMed: 16598726]
49. Haacke EM, Lai S, Reichenbach JR, Kuppusamy K, Hoogenraad FG, Takeichi H, Lin W. In vivo measurement of blood oxygen saturation using magnetic resonance imaging: a direct validation of the blood oxygen level-dependent concept in functional brain imaging. Hum Brain Mapp. 1997; 5(5):341–346. [PubMed: 20408238]
50. He X, Yablonskiy DA. Quantitative BOLD: mapping of human cerebral deoxygenated blood volume and oxygen extraction fraction: default state. Magn Reson Med. 2007; 57(1):115–126. [PubMed: 17191227]
51. Jain V, Langham MC, Wehrli FW. MRI estimation of global brain oxygen consumption rate. J Cereb Blood Flow Metab. 2010; 30(9):1598–1607. [PubMed: 20407465]
52. Krishnamurthy LC, Liu P, Ge Y, Lu H. Vessel-specific quantification of blood oxygenation with T2-Relaxation-Under-Phase-Contrast (TRU-PC) MRI. Magn Reson in Med. in press.
53. Schmidt, S.; Petersen, ET.; Hendrikse, J.; Webb, A.; vanOsch, MJP. Improved selection of the venous blood pool for OEF determination: IQ-OEF. Melbourne, Australia: 2012. p. 2008
54. Christen T, Lemasson B, Pannetier N, Farion R, Segebarth C, Remy C, Barbier EL. Evaluation of a quantitative blood oxygenation level-dependent (qBOLD) approach to map local blood oxygen saturation. NMR Biomed. 2010; 24(4):393–403. [PubMed: 20960585]
55. Yablonskiy DA, Haacke EM. Theory of NMR signal behavior in magnetically inhomogeneous tissues: the static dephasing regime. Magn Reson Med. 1994; 32(6):749–763. [PubMed: 7869897]
56. Bulte DP, Kelly M, Germuska M, Xie J, Chappell MA, Okell TW, Bright MG, Jezzard P. Quantitative measurement of cerebral physiology using respiratory-calibrated MRI. Neuroimage. 2012; 60(1):582–591. [PubMed: 22209811]
57. Gauthier CJ, Hoge RD. Magnetic resonance imaging of resting OEF and CMRO(2) using a generalized calibration model for hypercapnia and hyperoxia. Neuroimage. 2011; 60(2):1212–1225. [PubMed: 22227047]
58. Gauthier CJ, Hoge RD. A generalized procedure for calibrated MRI incorporating hyperoxia and hypercapnia. Hum Brain Mapp. in press; doi: 10.1002/hbm.21495.
59. Haacke EM, Cheng NY, House MJ, Liu Q, Neelavalli J, Ogg RJ, Khan A, Ayaz M, Kirsch W, Obenaus A. Imaging iron stores in the brain using magnetic resonance imaging. Magn Reson Imaging. 2005; 23(1):1–25. [PubMed: 15733784]
60. Teeuwisse WM, Brink WM, Webb AG. Quantitative assessment of the effects of high-permittivity pads in 7 Tesla MRI of the brain. Magn Reson Med. 2012; 67(5):1285–1293. [PubMed: 21826732]

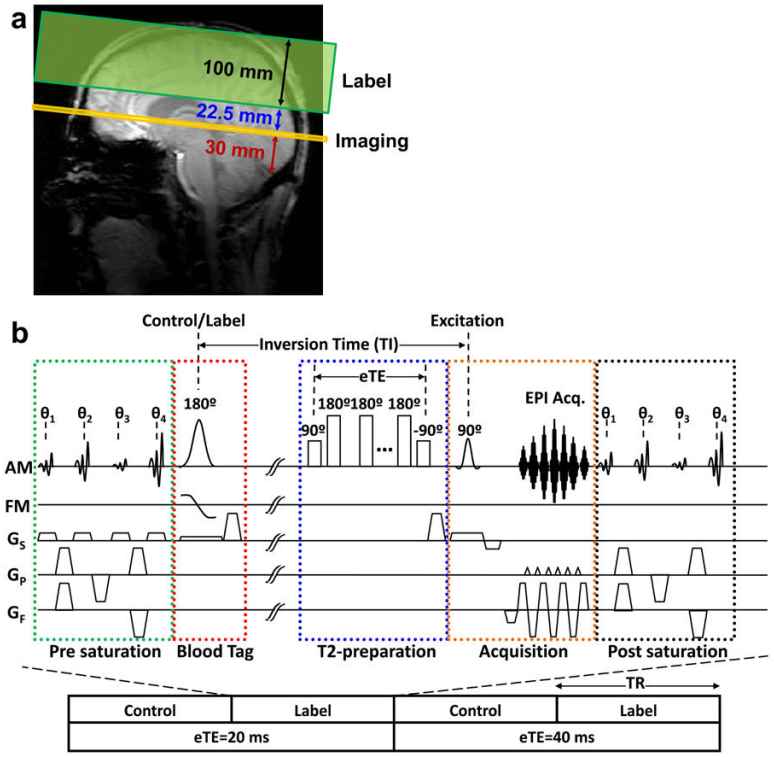

Figure 1.

Description of the methods used for *in vivo* quantification of blood T_2. (a) Slice positioning of the T_2-Relaxation-Under-Spin-Tagging (TRUST) scan. (b) Pulse sequence diagram of TRUST MRI. A complete data set includes control and label images acquired at two different T_2-preparation durations (referred to as effective TE, eTE). In practice, 16 repetitions are used.

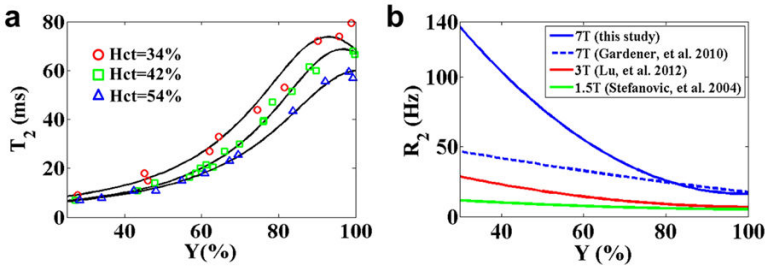

Figure 2.

Results of the *in vitro* study on blood samples. (a) Blood T_2 is plotted as a function of Y for three different Hct levels used in the experiments. The solid lines show the fitted curves based on Equation [1]. (b) Comparison of blood R_2 (=1/T_2) at 7T with literature reports at 1.5T and 3T, where Hct = 0.51. 1.5T data were based on Stefanovic et al. (13). 3T data were based on Lu et al. (26). At each field strength, R_2 is plotted as a function of Y. Also plotted are results from an earlier report of blood R_2 at 7T (11).

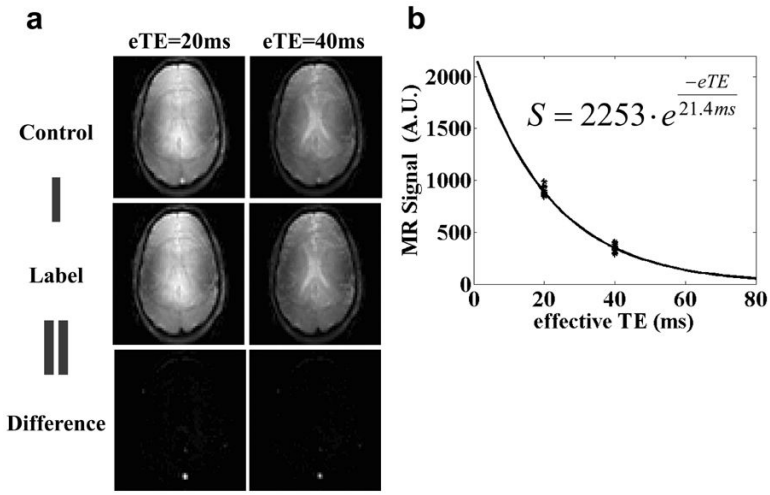

Figure 3.

A representative set of images for the TRUST MRI scan at 7T. (a) Control and Label images at two eTEs. The posterior portions of the “Control” images show a bright blood signal in the region of the superior sagittal sinus. This signal is suppressed in the “Label” images. The “Difference” image is the subtraction of “Label” from the “Control” image, removing tissue signal and leaving pure blood signal. (b) “Difference” signal as a function of eTE. There are 16 data points for each eTE. The solid line shows the fitted curve. The fitted equation is also listed.

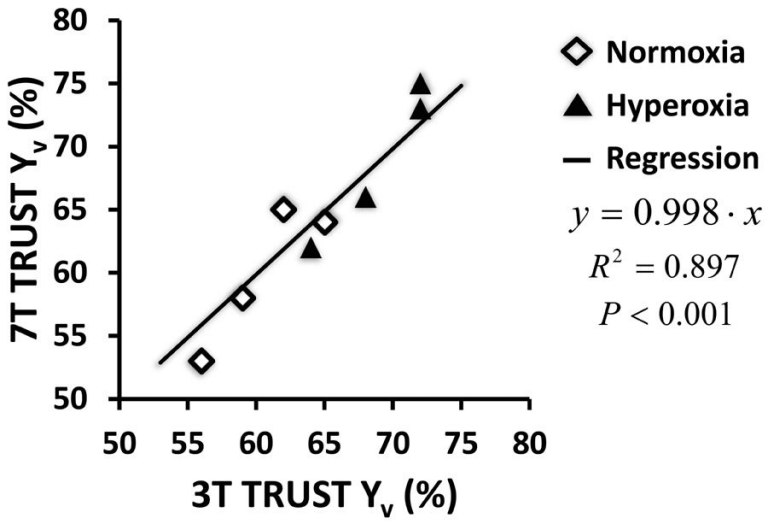

Figure 4.

A scatter plot of correlation between TRUST data at 7T and at 3T. The data were obtained from a group of four subjects. Each subject contributed two data points to the plot, one during normoxia (open diamond symbols) and the other duration hyperoxia (filled triangle symbols).

Table 1

Fitted values of coefficients in Equation [1]. The coefficients were obtained by fitting the experimental data to Equation [1] at each hematocrit. Linear interpolation of each coefficient can be used to describe T_2-relaxometry at other Hct values.

Hct	A	B	C
34%	14.6	−31.2	223.5
42%	14.9	−17.6	264.0
54%	16.7	3.7	240.9

Table 2

Physiologic responses to hyperoxia challenge at 3T and 7T (Mean ± STD, N=4).

	Normoxia				Hyperoxia			
B_0	EtO_2	$EtCO_2$	T_2	Y_v	EtO_2	$EtCO_2$	T_2	T_v
3T	135±3	41±3	60.3±5.9	60.5±3.6	697±6	39±2	77.2±8.3	68.9±3.7
7T	133±2	41±3	20.5±4.3	60.0±5.6	701±2	38±2	29.7±6.9	69.0±6.1

B_0 – field strength, EtO_2 – end-tidal O_2 (mmHg), $EtCO_2$ – end-tidal CO_2 (mmHg), T_2 – *in vivo* blood T_2 (ms), Y_v – venous blood oxygenation (%).